

Colorless Top Partners, a 125 GeV Higgs, and the Limits on Naturalness

Gustavo Burdman,¹ Zackaria Chacko,² Roni Harnik,³
Leonardo de Lima,⁴ and Christopher B. Verhaaren²

¹*Instituto de Física, Universidade de São Paulo,
São Paulo, São Paulo 05508-900, Brazil*

²*Maryland Center for Fundamental Physics, Department of Physics,
University of Maryland, College Park, MD 20742-4111 USA*

³*Fermilab, P.O. Box 500, Batavia, IL 60510, USA*

⁴*Instituto de Física Teórica, Universidade Estadual Paulista,
São Paulo, São Paulo 01140-070, Brazil*

(Dated: March 5, 2015)

Abstract

Theories of physics beyond the Standard Model that address the hierarchy problem generally involve top partners, new particles that cancel the quadratic divergences associated with the Yukawa coupling of the Higgs to the top quark. With extensions of the Standard Model that involve new colored particles coming under strain from collider searches, scenarios in which the top partners carry no charge under the strong interactions have become increasingly compelling. Although elusive for direct searches, these theories predict modified couplings of the Higgs boson to the Standard Model particles. This results in corrections to the Higgs production and decay rates that can be detected at the Large Hadron Collider (LHC) provided the top partners are sufficiently light, and the theory correspondingly natural. In this paper we consider three theories that address the little hierarchy problem and involve colorless top partners, specifically the Mirror Twin Higgs, Folded Supersymmetry, and the Quirky Little Higgs. For each model we investigate the current and future bounds on the top partners, and the corresponding limits on naturalness, that can be obtained from the Higgs program at the LHC. We conclude that the LHC will not be able to strongly disfavor naturalness, with mild tuning at the level of about one part in ten remaining allowed even with 3000 fb^{-1} of data at 14 TeV.

I. INTRODUCTION – UNCOLORED TOP PARTNERS

“It’s a bit like spotting a familiar face from afar. Sometimes you need closer inspection to find out whether it’s really your best friend, or actually your best friend’s twin.”

– *Rolf Heuer, July 2012*

The discovery of a 125 GeV Higgs boson at the LHC [1, 2] seems to complete the Standard Model (SM) of particle physics. With the inclusion of the Higgs, the SM is a perfectly well-behaved theory up to energies that are exponentially higher than the Higgs mass. This extrapolation, without the inclusion of new physics, presents a theoretical problem because achieving the observed hierarchy between the electroweak scale and the Planck scale requires exquisite fine-tuning. This tuning is required because quadratically divergent radiative corrections to the Higgs mass parameter need to be canceled by a large bare mass. One of the most important questions in high energy physics today is whether such a tuning indeed exists in nature or whether the electroweak scale is set by a mechanism that does not require a large cancellation. This is the question of Higgs naturalness, or the hierarchy problem.

An attractive dynamical solution to the naturalness problem is to posit a new symmetry which protects the Higgs against large radiative corrections. Invoking such a symmetry implies the existence of particles beyond the SM which constitute the “symmetry partners” of known SM fields. Considered from the bottom up, the hierarchy problem is dominated by the one loop diagram involving the top quark. Any model that addresses the hierarchy problem must therefore include symmetry partners for the top quark, the “top partners.” To avoid significant residual tuning, the top partners are expected to have masses at or below the TeV scale. Well known examples of top partners include the scalar stops in supersymmetric models (for a review see [3]) and vectorlike fermionic top-primes in little Higgs models [4–7] (for a review see [8]). In these examples the new symmetry that is protecting the Higgs commutes with the SM gauge symmetries, and so the top partners have identical quantum numbers to those of the top. In particular, the top partners in

these models are charged under the SM color group. This fact, in combination with the expectation that these particles lie at or below the TeV scale, leads to the conclusion that top partners should be produced at the LHC with high rates.

Searches for colored top partners, both scalar and fermionic, have so far yielded only stringent limits (see e.g. [9–12]). Broadly speaking, their masses are constrained to lie above around 700 GeV. This limit is by no means model independent. Indeed, top partners could be hiding, for example, in R-parity violating supersymmetric models, if the spectrum is squeezed [13], or in more elaborate constructions [14]. As the LHC experiments improve their analyses, the expectation is that most of these holes in the search for natural models will be covered.

As models of new physics in which the top partners are colored come under increasing strain from LHC searches, theories in which the top partners are *not* charged under the strong interactions appear ever more compelling. Colorless top partners arise in scenarios where the symmetry that protects the Higgs mass does not commute with the SM $SU(3)$ color group [15–18]. Instead, the action of the symmetry is to interchange SM color with a hidden color group, labeled QCD' .

In such a framework, the phenomenology associated with the top partners is strikingly different. In particular, since the production cross sections for uncolored top partners are many orders of magnitude smaller than in the colored case, this allows a simple understanding of why these particles have so far escaped discovery.

The most striking possibility along these lines is the Mirror Twin Higgs model, where the Higgs is protected by the discrete Z_2 subgroup of a larger global symmetry [15] (see also [19–23]). The matter content of the theory is simply the SM, and an additional mirror, or twin, copy of the SM. In such a scenario, *all of the new particles which ensure Higgs naturalness up to scales of order 5-10 TeV are singlets under the SM*. The only way to produce new particles at the LHC, or to see their effects, is through the Higgs boson itself. In this case, the effects of new physics might only appear in precision Higgs measurements. While more exotic signals, such as the displaced vertices characteristic of hidden valleys [24], are certainly possible in specific realizations of this scenario, they are by no means guaranteed. It is therefore important to study the Higgs phenomenology of this framework in detail.

In other scenarios, the top partners, while remaining uncolored, carry electroweak (EW) charges in addition to QCD' . Examples of such theories include Folded Supersymmetry [16]

and the Quirky Little Higgs [18]. In such a scenario the top partners may be directly produced through the weak interactions. In these theories there are no fermions or scalars with masses below the scale where QCD' gets strong. Therefore the top partners, once produced, exhibit quirky dynamics [25], which leads them to lose energy to radiation, followed by pair annihilation [25–27]. As a consequence of the low EW production rates and the exotic phenomenology, discovering these states directly is challenging and may require a large LHC data set. Therefore, in such scenarios it is also important to study the effects of such models on Higgs production and decay rates, since this may lead to stronger limits. A study of the Higgs physics would also be important in establishing that the quirks, once discovered, are involved in addressing the hierarchy problem.

A different category of models is one in which the top partners carry electroweak charges, but the gauge symmetry corresponding to QCD' is broken and is not present at low energies. This is the case in the Dark Top model [17], which has the interesting feature that the top partners also constitute the observed dark matter.

In this work we consider some specific theories where the top partners are colorless, and study the phenomenology associated with the Higgs. In what follows we consider in turn three models: the Mirror Twin Higgs in Section II, Folded Supersymmetry in Section III, and the Quirky Little Higgs in Section IV. For each case we obtain expressions for the Higgs production cross section in various channels, and the branching ratios into various final states. We use this to determine the current and future bounds on the top partners, and the corresponding limits on naturalness, that can be obtained from the Higgs program at the LHC.

II. MIRROR TWIN HIGGS

A. The Model and Cancellation Mechanism

The Mirror Twin Higgs (MTH) model assumes a mirror copy of the complete SM, called the twin sector, along with a Z_2 symmetry that exchanges each SM particle with the corresponding twin partner. In addition, the Higgs sector of the theory is assumed to respect an approximate global symmetry, which may be taken to be either $SU(4) \times U(1)$ or $O(8)$. This global symmetry is not exact, but is explicitly violated by the SM Yukawa couplings,

and also by the SM electroweak gauge interactions. In particular, a subgroup of this global symmetry is gauged, and contains the $SU(2) \times U(1)$ electroweak interactions of the SM, and of the twin sector. The SM Higgs doublet emerges as a light pseudo-Nambu-Goldstone boson (pNGB) when the global symmetry is spontaneously broken. In spite of the fact that the gauge and Yukawa interactions explicitly violate the global symmetry, the discrete Z_2 symmetry ensures the absence of quadratically divergent contributions to the Higgs mass to one loop order.

The next step is to understand the cancellation of the quadratic divergences in this model. We first consider the case where the breaking of the global symmetry, which for concreteness we take to be $SU(4) \times U(1)$, is realized by a weakly coupled Higgs sector. The $SU(2) \times SU(2) \times U(1)$ subgroup of $SU(4)$ and the additional $U(1)$ are gauged giving rise to the electroweak interactions in the SM and twin sectors. We use the labels A and B to denote the SM and twin sectors respectively. Then, under the action of the discrete Z_2 symmetry, the labels A and B are interchanged, $A \leftrightarrow B$. In this notation, H_A represents the SM Higgs doublet and H_B the twin doublet. The field H , defined as

$$H = \begin{pmatrix} H_A \\ H_B \end{pmatrix}, \quad (1)$$

is chosen to transform as the fundamental representation under the global $SU(4)$ symmetry. The $SU(4)$ invariant potential for H takes the form

$$m^2 H^\dagger H + \lambda (H^\dagger H)^2 \quad (2)$$

If the parameter m^2 is negative, the $SU(4) \times U(1)$ symmetry is spontaneously broken to $SU(3) \times U(1)$ and there are 7 massless NGBs in the spectrum. Depending on the alignment of the vacuum expectation value (VEV), several of these NGBs will be eaten. If, however, the VEV of H lies along H_B , the SM Higgs doublet H_A will remain massless.

The gauge and Yukawa interactions give rise to radiative corrections that violate the global symmetry and generate a mass for H_A . We focus on the top Yukawa coupling, which takes the form

$$\lambda_A H_A q_A t_A + \lambda_B H_B q_B t_B. \quad (3)$$

These interactions generate quadratically divergent corrections to the Higgs potential at one

loop order. The corrections take the form

$$\Delta V = \frac{3}{8\pi^2} \Lambda^2 \left(\lambda_A^2 H_A^\dagger H_A + \lambda_B^2 H_B^\dagger H_B \right) , \quad (4)$$

where Λ is the ultraviolet (UV) cutoff. The Z_2 symmetry, however, ensures $\lambda_A = \lambda_B \equiv \lambda$ so that

$$\Delta V = \frac{3\lambda^2}{8\pi^2} \Lambda^2 \left(H_A^\dagger H_A + H_B^\dagger H_B \right) = \frac{3\lambda^2}{8\pi^2} \Lambda^2 H^\dagger H . \quad (5)$$

Thus, this contribution respects the global symmetry and so cannot contribute to the mass of the NGBs. The leading contributions to the SM Higgs potential therefore arise from terms which are only logarithmically divergent. Consequently, there are no quadratically divergent contributions to the Higgs mass at one loop order.

The discussion so far has been restricted to the case when the breaking of the global symmetry is realized by a weakly coupled Higgs sector. However, the cancellation is in fact independent of the specifics of the UV completion and depends only on the symmetry breaking pattern. To see this we consider the low energy effective theory for the light degrees of freedom, in which the symmetry is realized nonlinearly. We parametrize the pNGB degrees of freedom in terms of fields $\Pi^a(x)$ that transform nonlinearly under the broken symmetry. For the purpose of writing interactions, it is convenient to define an object H which transforms linearly under $SU(4) \times U(1)$,

$$H = \begin{pmatrix} H_A \\ H_B \end{pmatrix} = \exp \left(\frac{i}{f} \Pi \right) \begin{pmatrix} 0 \\ 0 \\ 0 \\ f \end{pmatrix} . \quad (6)$$

Here f is the symmetry breaking VEV, and Π is given, in unitary gauge where all the B sector NGBs have been eaten by the corresponding vector bosons, by

$$\Pi = \left(\begin{array}{ccc|c} 0 & 0 & 0 & h_1 \\ 0 & 0 & 0 & h_2 \\ 0 & 0 & 0 & 0 \\ \hline h_1^* & h_2^* & 0 & 0 \end{array} \right) . \quad (7)$$

The discrete Z_2 symmetry continues to interchange H_A and H_B . Expanding out the expo-

nential we obtain

$$H = \begin{pmatrix} \mathbf{h} \frac{if}{\sqrt{\mathbf{h}^\dagger \mathbf{h}}} \sin\left(\frac{\sqrt{\mathbf{h}^\dagger \mathbf{h}}}{f}\right) \\ 0 \\ f \cos\left(\frac{\sqrt{\mathbf{h}^\dagger \mathbf{h}}}{f}\right) \end{pmatrix} \quad (8)$$

where $\mathbf{h} = (h_1, h_2)^T$ is the Higgs doublet of the SM

$$H_A = \mathbf{h} \frac{if}{\sqrt{\mathbf{h}^\dagger \mathbf{h}}} \sin\left(\frac{\sqrt{\mathbf{h}^\dagger \mathbf{h}}}{f}\right) = i\mathbf{h} + \dots, \quad (9)$$

$$H_B = \begin{pmatrix} 0 \\ f \cos\left(\frac{\sqrt{\mathbf{h}^\dagger \mathbf{h}}}{f}\right) \end{pmatrix} = \begin{pmatrix} 0 \\ f - \frac{1}{2f} \mathbf{h}^\dagger \mathbf{h} + \dots \end{pmatrix}. \quad (10)$$

Now consider again the Z_2 symmetric top quark sector, Eq. 3. To quadratic order in \mathbf{h} this takes the form

$$i\lambda_t \mathbf{h} q_A t_A + \lambda_t \left(f - \frac{1}{2f} \mathbf{h}^\dagger \mathbf{h} \right) q_B t_B. \quad (11)$$

From this Lagrangian, we can evaluate the radiative contributions to the Higgs mass parameter. The contributing diagrams are shown in Fig. 1.

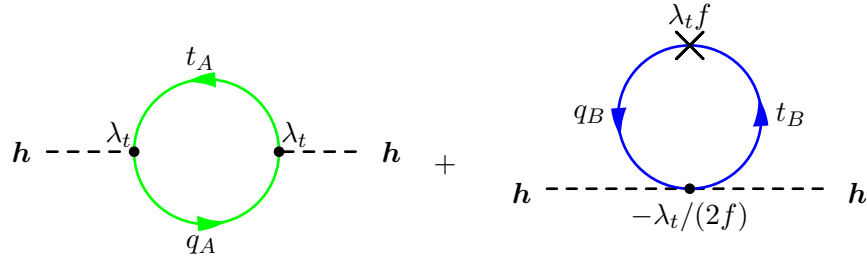


FIG. 1. Cancellation of quadratic divergences in the Mirror Twin Higgs model. The cancellation holds when the top and its partner are charged under different $SU(3)$ s.

Evaluating these diagrams we find that the quadratic divergence arising from the first diagram is exactly canceled by that of the second. The first and second diagrams have been colored differently to emphasize that the particles running in the two loops carry different $SU(3)$ charges. The first loop has the SM top quarks which carry SM color. The particles running in the second loop, however, are twin top quarks charged under twin color, not SM color.

B. Effects on Higgs Physics

In order to understand the implications of this model for Higgs production and decays, we first determine the couplings of the Higgs to the states in the low energy theory. We choose the unitary gauge in the visible sector with $h_1 = 0$ and $h_2 = (v + \rho)/\sqrt{2}$ to obtain

$$H_A = \begin{pmatrix} 0 \\ if \sin\left(\frac{v + \rho}{\sqrt{2}f}\right) \end{pmatrix}, \quad H_B = \begin{pmatrix} 0 \\ f \cos\left(\frac{v + \rho}{\sqrt{2}f}\right) \end{pmatrix}. \quad (12)$$

The couplings of the weak gauge bosons to the Higgs spring from

$$|D_\mu^A H_A|^2 + |D_\mu^B H_B|^2 \quad (13)$$

where the $D^{A,B}$ denote the covariant derivative employing the A, B gauge bosons. Expanding out the kinetic terms we find

$$\begin{aligned} \frac{1}{2} \partial_\mu \rho \partial^\mu \rho + & \left[\frac{f^2 g^2}{2} W_{A\mu}^+ W_A^{\mu-} + \frac{f^2 g^2}{4 \cos^2 \theta_W} Z_{A\mu} Z_A^\mu \right] \sin^2 \left(\frac{v + \rho}{\sqrt{2}f} \right) \\ & + \left[\frac{f^2 g^2}{2} W_{B\mu}^+ W_B^{\mu-} + \frac{f^2 g^2}{4 \cos^2 \theta_W} Z_{B\mu} Z_B^\mu \right] \cos^2 \left(\frac{v + \rho}{\sqrt{2}f} \right). \end{aligned} \quad (14)$$

From this we obtain the masses of the W^\pm and Z gauge bosons in the visible and twin sectors and their couplings to the Higgs, ρ . We find that

$$m_{W_A}^2 = \frac{f^2 g^2}{2} \sin^2 \left(\frac{v}{\sqrt{2}f} \right), \quad m_{W_B}^2 = \frac{f^2 g^2}{2} \cos^2 \left(\frac{v}{\sqrt{2}f} \right). \quad (15)$$

The masses of the Z bosons are related to those of the W s by the usual factor of $\cos \theta_W$. Notice that the VEV of the Higgs in the SM, $v_{\text{EW}} = 246$ GeV, is related to the parameters v and f of the MTH model by the relation

$$v_{\text{EW}} = \sqrt{2}f \sin \left(\frac{v}{\sqrt{2}f} \right) \equiv \sqrt{2}f \sin \vartheta. \quad (16)$$

From this expression, which defines the angle ϑ , we see that v and v_{EW} become equal in the $v \ll f$, or equivalently $\vartheta \ll 1$, limit.

In the absence of any effects that violate the Z_2 symmetry, minimization of the Higgs potential will reveal that $v_{\text{EW}} = f$, so that the state ρ is composed of visible and hidden sector states in equal proportions. In order to avoid the experimental limits on this scenario, it is desirable to create a hierarchy between these scales so that $v_{\text{EW}} < f$. This is most simply

realized by a soft explicit breaking of the Z_2 symmetry. This allows the gauge and Yukawa couplings to remain the same across the A and B sectors, so that the cancellation of quadratic divergences remains intact.

We can expand out (14) to obtain the couplings of the Higgs to the electroweak gauge bosons

$$\begin{aligned} \frac{1}{2} \partial_\mu \rho \partial^\mu \rho + & \left[m_{W_A}^2 W_{A\mu}^+ W_A^{\mu-} + \frac{m_{Z_A}^2}{2} Z_{A\mu} Z_A^\mu \right] \left(1 + 2 \frac{\rho}{v_{EW}} \cos \vartheta + \dots \right) \\ & + \left[m_{W_B}^2 W_{B\mu}^+ W_B^{\mu-} + \frac{m_{Z_B}^2}{2} Z_{B\mu} Z_B^\mu \right] \left(1 - 2 \frac{\rho}{v_{EW}} \tan \vartheta \sin \vartheta + \dots \right). \end{aligned} \quad (17)$$

We see that the couplings of ρ to the W and Z differ by a factor of $\cos \vartheta$ from the SM prediction.

We now turn to the top quark sector (3). Expanding this in the unitary gauge we find

$$\begin{aligned} & \lambda_t \left[i f q_A t_A \sin \left(\frac{v + \rho}{\sqrt{2} f} \right) + f q_B t_B \cos \left(\frac{v + \rho}{\sqrt{2} f} \right) \right] \\ & = i \frac{\lambda_t v_{EW}}{\sqrt{2}} q_A t_A \left[1 + \frac{\rho}{v_{EW}} \cos \vartheta \right] + \lambda_t f q_B t_B \cos \vartheta \left[1 - \frac{\rho}{v_{EW}} \tan \vartheta \sin \vartheta \right] \end{aligned} \quad (18)$$

where for simplicity we have not differentiated the components in the SU(2) doublets. We also see that the mass of the top quark's mirror twin partner is

$$m_T = \lambda_t f \cos \vartheta = m_t \cot \vartheta. \quad (19)$$

We are also in a position to determine the implications of the MTH model for Higgs production and decays. We have seen that the tree level couplings of ρ to the visible sector fermions and bosons are simply altered by a factor $\cos \vartheta$ relative to the SM. Since the new particles in the model carry no SM charges, the radiatively generated couplings of the Higgs to gluons and photons are modified relative to the SM by exactly the same factor. It follows that all production cross sections are modified by the square of this factor,

$$\sigma(pp \rightarrow \rho) = \cos^2 \vartheta \sigma_{SM}(pp \rightarrow h) \quad (20)$$

where h is the SM Higgs boson. There is a similar relation for decays of the Higgs into A sector particles,

$$\Gamma(\rho \rightarrow A_i) = \Gamma^{SM}(h \rightarrow SM_i) \cos^2 \vartheta, \quad (21)$$

where the subscript i represents any particle species. In addition, ρ will decay into B sector particles that are light enough. A factor of $\sin \vartheta$ accompanies couplings of ρ to twin sector

states, relative to the corresponding SM interactions. We define the fraction δ as

$$\delta = \frac{\Gamma(\rho \rightarrow B)}{\Gamma^{\text{SM}}(h) \sin^2 \vartheta} . \quad (22)$$

In the limit that the states in the twin sector have the same masses as their visible sector partners, $\delta = 1$. Away from this limit, δ is expected to differ from unity due to kinematic effects. The total Higgs width in the MTH model is given by

$$\Gamma(\rho) = \Gamma^{\text{SM}}(h) [\cos^2 \vartheta + \delta \sin^2 \vartheta] . \quad (23)$$

Employing the expressions $\Gamma_{\text{BR}}^{\text{SM}}(h \rightarrow \text{SM}_i)$ and $\Gamma_{\text{BR}}(\rho \rightarrow A_i)$ to denote the branching fractions into the same particle species i we obtain

$$\frac{\sigma(pp \rightarrow \rho) \Gamma_{\text{BR}}(\rho \rightarrow A_i)}{\sigma_{\text{SM}}(pp \rightarrow h) \Gamma_{\text{BR}}^{\text{SM}}(h \rightarrow \text{SM}_i)} = \frac{\cos^2 \vartheta}{1 + \delta \tan^2 \vartheta} = \frac{1}{\left(1 + \delta \frac{m_t^2}{m_T^2}\right) \left(1 + \frac{m_t^2}{m_T^2}\right)} . \quad (24)$$

As explained earlier, in the case when the Z_2 symmetry is only softly broken, the gauge and Yukawa couplings are the same in the visible and twin sectors. This allows us to obtain expressions for the masses of the particles in the twin sector, and predict δ . The masses of the B sector particles are related to those in the A sector by

$$m_B = m_A \cot \vartheta \quad (25)$$

and so for $f \gg v$ the B sector masses are significantly larger than those of the A sector. The B sector particles couple to ρ with the same coupling as in the SM, but modified by the factor $-\sin \vartheta$.

The leading order relation for SM Higgs decays to fermions f is given by

$$\Gamma(h \rightarrow f\bar{f}) = \frac{N_c}{16\pi} m_h \lambda_f^2 \left(1 - 4 \frac{m_f^2}{m_h^2}\right)^{3/2} , \quad (26)$$

where λ_f is to be evaluated at the Higgs mass. For decays into gauge bosons we use [28]

$$\Gamma(h \rightarrow VV^*) = \frac{3m_h}{32\pi^3} \frac{m_V^4}{v_{\text{EW}}^4} \delta_V R_T \left(\frac{m_V^2}{m_H^2}\right) \quad (27)$$

where $\delta'_W = 1$, $\delta'_Z = \frac{7}{12} - \frac{10}{9} \sin^2 \theta_W + \frac{40}{9} \sin^4 \theta_W$, and

$$\begin{aligned} R_T(x) = & \frac{3(1 - 8x + 20x^2)}{\sqrt{4x - 1}} \cos^{-1} \left(\frac{3x - 1}{2x^{3/2}} \right) - \frac{1 - x}{2x} (2 - 13x + 47x^2) \\ & - \frac{3}{2} (1 - 6x + 4x^2) \ln x \end{aligned} \quad (28)$$

when the mass of the vector is less than the mass of the Higgs. By suitably modifying these expressions, we can obtain the width of the Higgs into twin fermions and twin electroweak gauge bosons. The Higgs may also decay into twin gluons g_B :

$$\Gamma(\rho \rightarrow g_B g_B) = \frac{\alpha_s^2 m_h^3}{72\pi^3 v^2} \left| \frac{3}{4} \sum_q A_F \left(\frac{4m_q^2}{m_h^2} \right) \right|^2 \quad (29)$$

with A_F defined in (A6). The sum is over the twin quarks, but is dominated by the twin top.

We use these formulas in conjunction with the factor of $\sin^2 \vartheta$ to determine δ as a function of m_t/m_T :

$$\begin{aligned} \delta = & \sum_j \Gamma_{\text{BR}}^{\text{SM}}(h \rightarrow f_j \bar{f}_j) \left[\frac{1 - 4 \frac{m_{f_j}^2}{m_h^2} \frac{m_T^2}{m_t^2}}{1 - 4 \frac{m_{f_j}^2}{m_h^2}} \right]^{3/2} + \sum_j \Gamma_{\text{BR}}^{\text{SM}}(h \rightarrow V_j V_j^*) \frac{R_T \left(\frac{m_{V_j}^2}{m_h^2} \frac{m_T^2}{m_t^2} \right)}{R_T \left(\frac{m_{V_j}^2}{m_h^2} \right)} \\ & + \Gamma_{\text{BR}}^{\text{SM}}(h \rightarrow gg) \frac{\left| A_F \left(\frac{4m_T^2}{m_h^2} \right) \right|^2}{\left| A_F \left(\frac{4m_t^2}{m_h^2} \right) \right|^2} \end{aligned} \quad (30)$$

In our analysis, we take into account the decay modes of ρ into the twin sector bottom and charm quarks, and into the tau and muon leptons. We use the Higgs widths reported in [29].

Using these results we can determine the rate of Higgs events into any SM state and the branching fraction into twin sector states. We plot these results in Fig. 2. The blue line represents the rate of Higgs events into SM final states in the softly broken MTH model normalized to the SM. The green line denotes the branching fraction of the Higgs into the twin sector particles. A key observation is that the MTH model predicts a relation between the Higgs invisible branching fraction and the modification to standard model rates.

The corrections to the Higgs couplings in the MTH model relative to the SM are constrained by precision electroweak measurements. In theories where the Higgs emerges as a pNGB, its couplings to the fermions and gauge bosons are generally smaller than in the SM. In [30] precision electroweak constraints were applied to the MCHM4 model [31], which, like MTH, modifies the Higgs couplings to all the vector bosons and fermions by a universal factor. Their bound on ϵ , where $\sqrt{1 - \epsilon^2} = \cos \vartheta$, also applies to the MTH model in a strongly coupled UV completion, and can be translated into a bound on the top partner

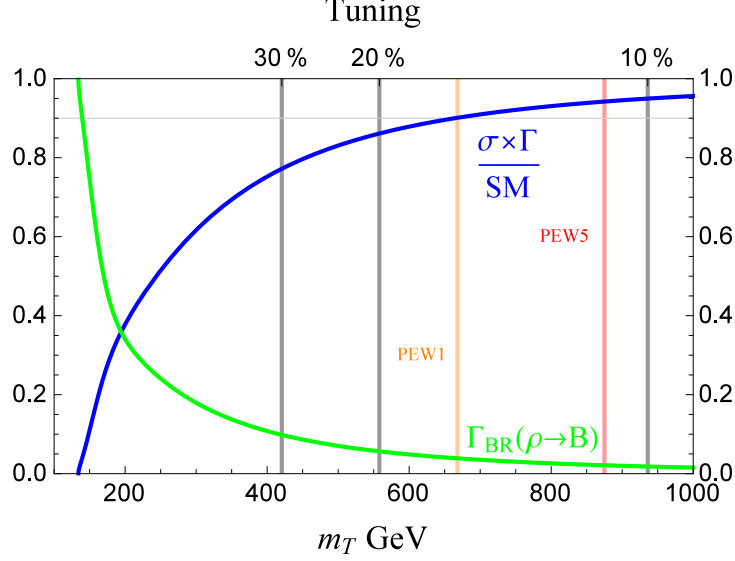


FIG. 2. In blue, a plot of the rate of Higgs events into SM states normalized to the SM. The green line is the invisible branching ratio of the Higgs into mirror twin particles. The vertical orange and red lines are the 95% confidence bound from precision electroweak constraints for a 1 and 5 TeV cutoff respectively.

mass. Their analysis was carried out assuming a cutoff $\Lambda = 3$ TeV. In general, however, the leading contributions to the oblique parameters go like

$$\alpha T \sim -\epsilon^2 \ln \left(\frac{\Lambda}{m_Z} \right), \quad \alpha S \sim \epsilon^2 \ln \left(\frac{\Lambda}{m_Z} \right), \quad (31)$$

where m_Z is the mass of the Z boson. For ϵ sufficiently small we expect these parameters to dominate the analysis. In that case we may translate the bound on ϵ at Λ to a bound on ϵ' at Λ' by

$$\epsilon^2 \ln \left(\frac{\Lambda}{m_Z} \right) = \epsilon'^2 \left(1 + \frac{\ln \left(\frac{\Lambda}{\Lambda'} \right)}{\ln \left(\frac{\Lambda'}{m_Z} \right)} \right) \ln \left(\frac{\Lambda'}{m_Z} \right) \equiv \epsilon'^2 \ln \left(\frac{\Lambda'}{m_Z} \right). \quad (32)$$

The 2σ bound on ϵ' can be translated into a limit on the top partner mass. In Fig. 2 we denote bound corresponding to a 1 and 5 TeV cutoff by the vertical orange and red lines respectively.

Finally, we estimate the tuning Δ_m of the Higgs mass parameter m^2 as a function of the top partner mass as a measure of the naturalness of the MTH model. We use the formula

$$\Delta_m = \left| \frac{2\delta m^2}{m_h^2} \right|^{-1} \quad (33)$$

to estimate the tuning. We have denoted the quantum corrections to the Higgs mass parameter as δm^2 and the physical Higgs mass as $m_h = 125$ GeV.

The diagrams in Fig. 1 lead to

$$|\delta m^2| = \frac{3\lambda_t^2 m_T^2}{8\pi^2} \ln \left(\frac{\Lambda^2}{m_T^2} \right), \quad (34)$$

up to finite effects. We take the cutoff Λ to be 5 TeV. In Fig. 2 we have denoted the top partner masses corresponding to 30%, 20%, and 10% tuning.

The results of Fig. 2 should be compared to our expectations for the precision at which the LHC will be able to constrain these couplings. Projections for the full high luminosity LHC run (3000 fb⁻¹) [32] show that the Higgs invisible branching fraction will be probed down to about 10%. The precision for the signal strengths in the cleanest Higgs channels, ZZ , WW , and $\gamma\gamma$, is projected to be around 5%. The visible signal strengths are thus a stronger constraint on the model and can probe a level of tuning of about 10% (although combining several channels may improve this sensitivity). The sensitivity at the end of Run II is only slightly worse. We conclude that models that are tuned at the level of one part in ten may be able to escape detection at the LHC.

III. FOLDED SUPERSYMMETRY

A. The Model and Cancellation Mechanism

Supersymmetry (SUSY) is perhaps the best known solution to the hierarchy problem. In supersymmetric theories every known particle is related by the symmetry to another particle with a different spin, called its superpartner. The gauge quantum numbers of each particle and its corresponding superpartner are identical. In supersymmetric extensions of the SM, the quadratically divergent contributions to the Higgs mass from loops involving the SM particles are canceled by new diagrams involving the superpartners.

In the case of the top quark, whose left and right components belong to the SU(2) doublet q and SU(2) singlet u , the corresponding scalar partners are the scalar stops, which we label by \tilde{q} and \tilde{u} . Supersymmetric extensions of the SM generally contain two Higgs doublets, one labeled H_u which gives mass to the up-type quarks and another, labeled H_d , which gives mass to the down-type quarks and leptons. Both H_u and H_d have fermionic superpartners, the Higgsinos. In supersymmetric theories, the one loop quadratically divergent contributions to

the up-type Higgs mass associated with the top Yukawa coupling are canceled by diagrams involving the stops. The relevant couplings take the form

$$(\lambda_t H_u q u + \text{h.c.}) + \lambda_t^2 |\tilde{q} H_u|^2 + \lambda_t^2 |\tilde{u}|^2 |H_u|^2 . \quad (35)$$

These interactions lead to radiative corrections to the up-type Higgs mass from the diagrams shown in Fig. 3.

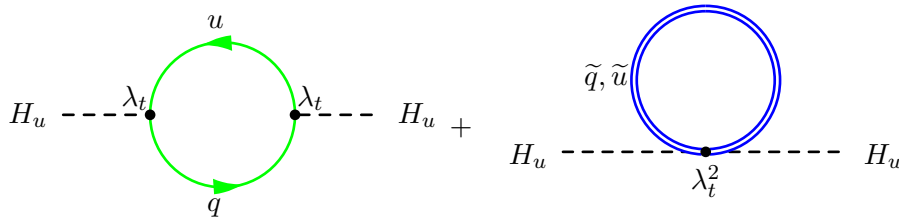


FIG. 3. Cancellation of quadratic divergences in the Folded SUSY model. This divergence is canceled even if the top and stop transform under different color groups.

From the form of the interaction in (35), we see that for the cancellation to go through, the left-handed stop \tilde{q} must carry charge under the $SU(2)$ gauge interactions of the SM. At the diagrammatic level, however, the cancellation does not depend on whether the stops transform under SM color.

In Folded Supersymmetric theories the cancellation of the one loop quadratic divergences associated with the top Yukawa coupling takes place exactly as in the diagrams above, but the top and its scalar partners, labeled “folded stops” or “F-stops”, are charged under different color groups. While the fermions transform under the familiar SM color group, now labeled $SU(3)_A$, the scalars transform under a separate hidden color group, labeled $SU(3)_B$. The electroweak quantum numbers of the F-stops are identical to those of the corresponding SM fermions. This scenario can be realized in a 5D supersymmetric construction, with the extra dimension compactified on S^1/Z_2 (see [33] for an alternative UV completion). A combination of boundary conditions and discrete symmetries ensures that the spectrum of light states includes the SM particles and the scalar folded superpartners (“F-spartners”) that cancel the quadratic divergences arising from the couplings of SM fermions to the up- and down-type Higgs bosons. The gauginos are projected out by the boundary conditions, and are not part of the low energy spectrum. The interactions of the top quarks and the F-stops with the up-type Higgs have exactly the same form as in (35), and the cancellation

of quadratic divergences between the fermion and scalar diagrams happens exactly the same way.

B. Effects on Higgs Physics

In general, the low energy spectrum of Folded Supersymmetry contains two Higgs doublets. Our analysis in this section will focus on the limit when one of the doublets is much lighter than the other, so that the corrections to the Higgs phenomenology primarily arise from the effects of the F-stops. In our discussion we follow the conventions of Haber[34]. In particular, we take $v_{\text{EW}} = \sqrt{v_d^2 + v_u^2} = 246$ GeV where v_u and v_d are the VEVs of the up-type and down-type Higgs fields respectively. The ratio of the up-type and down-type Higgs VEV is parametrized in terms of an angle β such that $\tan \beta = v_u/v_d$.

It is well known that in order to obtain a mass of 125 GeV for the light Higgs h^0 the MSSM is driven into a constrained parameter space with very heavy stops, resulting in significant tuning. This issue carries over to the folded SUSY construction. One of several possible ways to alleviate this constraint is to add another $U(1)_X$ gauge symmetry to the MSSM whose D -term contribution to the Higgs quartic increases the Higgs mass [35].

To be phenomenologically viable, the new gauge field Z' must have a mass $m_{Z'}$ not far above the scale of the soft masses [36]. This may be realized by giving two heavy scalar fields ϕ and ϕ^c VEVs that break the $U(1)_X$. The charge assignments of the SM fields under $U(1)_X$ are chosen to be the same as under hypercharge. After integrating out the ϕ fields the tree level Higgs quartic becomes

$$\frac{1}{8} \left[g_L^2 + g_Y^2 + g_X^2 \left(1 + \frac{m_{Z'}^2}{2m_\phi^2} \right)^{-1} \right] (|H_u|^2 - |H_d|^2)^2, \quad (36)$$

where g_L , g_Y , and g_X are the $SU(2)_L$, $U(1)_Y$, and $U(1)_X$ gauge groups. The mass m_ϕ is the soft mass of ϕ , which is chosen to be equal to that of ϕ^c for simplicity.

This method, while not the unique way to raise the Higgs mass, serves to illustrate that models of this type may have only moderate tuning from the top sector. For concreteness we pick g_X such that the Higgs mass, including one loop effects from the top and stops, is 125 GeV. For $m_{Z'} = 4$ TeV and $m_\phi = 5$ TeV a perturbative g_X can be chosen to give the correct Higgs mass. Additional details of the construction are given in Appendix B.

In the limit that only one Higgs doublet is light, its tree level couplings to the fermions and gauge bosons are necessarily of the same form as in the SM, up to small corrections. Therefore, we need only determine the couplings of the Higgs to the F-stops. The stop mixing matrix is given by

$$\begin{pmatrix} M_{\tilde{Q}}^2 + m_t^2 + m_Z^2 \left(\frac{1}{2} - \frac{2}{3}s_W^2 - \frac{1}{6}\hat{s}^2 \right) \cos 2\beta & m_t(A_t - \mu \cot \beta) \\ m_t(A_t - \mu \cot \beta) & M_{\tilde{U}}^2 + m_t^2 + m_Z^2 \frac{2}{3} \cos 2\beta (s_W^2 + \hat{s}^2) \end{pmatrix} \quad (37)$$

where $\sin \theta_W \equiv s_W$, $m_t = \lambda_t v_{EW} \sin(\beta)/\sqrt{2}$, and the effective coupling

$$\hat{s}^2 \equiv g_X^2 \left(1 + \frac{m_{Z'}^2}{2m_\phi^2} \right)^{-1} \frac{v_{EW}^2}{4m_Z^2}. \quad (38)$$

Although the original incarnation of Folded Supersymmetry has $A_t = 0$, in our analysis we allow for the possibility that there may be more general constructions that admit nonvanishing A_t . Then the heavy stop \tilde{T} and the light stop \tilde{t} can be written as

$$\tilde{T} = \cos \alpha_t \tilde{q} + \sin \alpha_t \tilde{u} \quad (39)$$

$$\tilde{t} = -\sin \alpha_t \tilde{q} + \cos \alpha_t \tilde{u} \quad (40)$$

where

$$\cos 2\alpha_t = \frac{M_{\tilde{Q}}^2 - M_{\tilde{U}}^2 + m_Z^2 \cos 2\beta \left(\frac{1}{2} - \frac{4}{3}s_W^2 - \frac{5}{6}\hat{s}^2 \right)}{m_{\tilde{T}}^2 - m_{\tilde{t}}^2}, \quad \sin 2\alpha_t = \frac{2m_t(A_t - \mu \cot \beta)}{m_{\tilde{T}}^2 - m_{\tilde{t}}^2}. \quad (41)$$

and

$$m_{\tilde{T}, \tilde{t}}^2 = \frac{1}{2} \left[M_{\tilde{Q}}^2 + M_{\tilde{U}}^2 + 2m_t^2 + \frac{1}{2}m_Z^2 \cos 2\beta (1 + \hat{s}^2) \right] \pm \frac{1}{2} \sqrt{\left[M_{\tilde{Q}}^2 - M_{\tilde{U}}^2 + m_Z^2 \cos 2\beta \left(\frac{1}{2} - \frac{4}{3}s_W^2 - \frac{5}{6}\hat{s}^2 \right) \right]^2 + 4m_t^2(A_t - \mu \cot \beta)^2}. \quad (42)$$

To ensure that the light stop \tilde{t} has non-negative mass the relation

$$m_t |A_t - \mu \cot \beta| \leq \sqrt{\left[M_{\tilde{Q}}^2 + m_t^2 + m_Z^2 \left(\frac{1}{2} - \frac{2}{3}s_W^2 - \frac{1}{6}\hat{s}^2 \right) \cos 2\beta \right] \left[M_{\tilde{U}}^2 + m_t^2 + m_Z^2 \frac{2}{3} \cos 2\beta (s_W^2 + \hat{s}^2) \right]} \quad (43)$$

must be satisfied.

We can then obtain the couplings of the heavy and light stop mass eigenstates to the light Higgs, $y_{\tilde{T}} h^0 |\tilde{T}|^2$ and $y_{\tilde{t}} h^0 |\tilde{t}|^2$. These are given by

$$y_{\tilde{T}} \equiv \frac{2}{v_{\text{EW}}} \left\{ m_t^2 + m_Z^2 \cos 2\beta \left[\frac{1}{4} + \frac{1}{4} \hat{s}^2 + \left(\frac{1}{4} - \frac{2}{3} s_W^2 - \frac{5}{12} \hat{s}^2 \right) \cos 2\alpha_t \right] + \frac{1}{2} m_t (A_t - \mu \cot \beta) \sin 2\alpha_t \right\}, \quad (44)$$

$$y_{\tilde{t}} \equiv \frac{2}{v_{\text{EW}}} \left\{ m_t^2 + m_Z^2 \cos 2\beta \left[\frac{1}{4} + \frac{1}{4} \hat{s}^2 - \left(\frac{1}{4} - \frac{2}{3} s_W^2 - \frac{5}{12} \hat{s}^2 \right) \cos 2\alpha_t \right] - \frac{1}{2} m_t (A_t - \mu \cot \beta) \sin 2\alpha_t \right\}. \quad (45)$$

We are now in a position to determine the Higgs phenomenology of this model. At tree level, the couplings of the Higgs to the fermions and to the W^\pm and Z gauge bosons are the same as in the SM model. Furthermore, since the F-stops carry no charge under SM color, the couplings of the Higgs to the gluons, which are generated at one loop, are also the same as in the SM. It follows that the Higgs production cross sections in the gluon fusion, associated production and vector boson fusion channels are largely unchanged from the SM predictions.

The Higgs decay widths into SM fermions, gluons and massive gauge bosons are also very close to the SM predictions. However, since the F-stops do carry electric charges, the rate of Higgs decays to two photons is affected. This can be used to constrain the model [37]. Using the results in Appendix A we find

$$\Gamma(h^0 \rightarrow \gamma\gamma) = \frac{\alpha^2 m_{h^0}^3}{1024\pi^3} \left| \frac{2}{v_{\text{EW}}} A_V \left(\frac{4m_W^2}{m_{h^0}^2} \right) + \frac{2}{v_{\text{EW}}} \frac{4}{3} A_F \left(\frac{4m_t^2}{m_{h^0}^2} \right) + \frac{y_{\tilde{t}}}{m_{\tilde{t}}^2} \frac{4}{3} A_S \left(\frac{4m_{\tilde{t}}^2}{m_{h^0}^2} \right) + \frac{y_{\tilde{T}}}{m_{\tilde{T}}^2} \frac{4}{3} A_S \left(\frac{4m_{\tilde{T}}^2}{m_{h^0}^2} \right) \right|^2 \quad (46)$$

where we have employed (44) and (45) to obtain the last two terms.

Having now accounted for all the decay modes we find the corrections to the total width are negligible. Therefore, we focus on only the diphoton channel. It can be seen from (44), (45) and (46) that in general the stop loops will contribute with the same sign as the top loops and therefore lead to a reduction in the diphoton decay rate. If the mixing A_t is increased, however, the coupling of the Higgs to the light stop can change sign, leading to an enhancement in the rate. We parametrize this difference from the SM value by

$$\delta = \frac{\Gamma(h^0 \rightarrow \gamma\gamma) - \Gamma^{\text{SM}}(h \rightarrow \gamma\gamma)}{\Gamma^{\text{SM}}(h \rightarrow \gamma\gamma)}. \quad (47)$$

Then, neglecting corrections to the overall Higgs width, we have

$$\frac{\sigma(pp \rightarrow h^0)\Gamma_{\text{BR}}(h^0 \rightarrow \gamma\gamma)}{\sigma_{\text{SM}}(pp \rightarrow h)\Gamma_{\text{BR}}^{\text{SM}}(h \rightarrow \gamma\gamma)} = 1 + \delta. \quad (48)$$

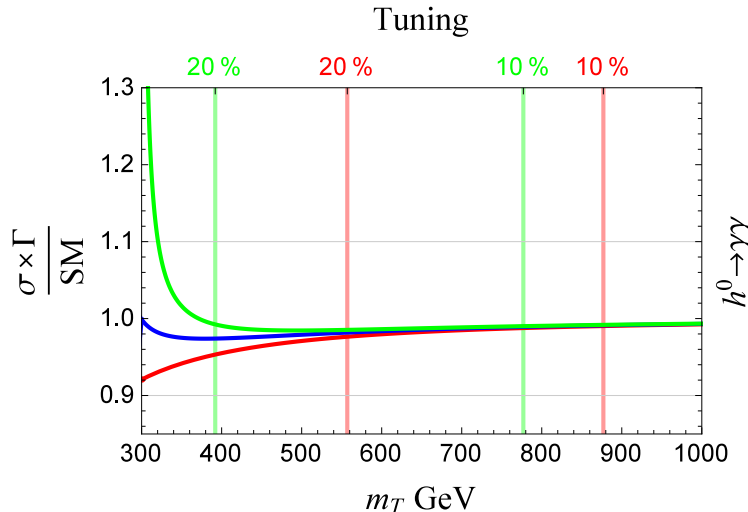


FIG. 4. Plots of the total Higgs to diphoton rate normalized to SM value as function of the square averaged stop mass m_T^2 . The red, blue, and green lines correspond to mixing $A_t - \mu \cot \beta$ equal to 100, 400, and 500 GeV. We have taken the soft masses equal, $\tan \beta = 10$, and $\mu = -200$ GeV. Contours of tuning are also plotted. The color of the contour indicates the size of A_t for which it applies.

In Fig. 4 we plot the total rate of the $h^0 \rightarrow \gamma\gamma$ normalized to the SM value as a function of the square averaged stop mass $m_T^2 = \frac{1}{2}(m_{\tilde{T}}^2 + m_t^2)$. For definiteness we take the stop soft masses to be equal, $\mu = -200$ GeV, and choose $\tan \beta = 10$. The red, blue, and green lines correspond to mixing terms $A_t - \mu \cot \beta$ equal to 100, 400, and 500 GeV respectively. We see that for small mixing the rate is reduced while for larger mixing the rate can be enhanced.

The tuning Δ_m of the Higgs mass parameter m^2 in this model differs only slightly from the MSSM case. As in the MTH model, we estimate the tuning as

$$\Delta_m = \left| \frac{2\delta m^2}{m_h^2} \right|^{-1} \quad (49)$$

where δm^2 represents the quantum corrections to the Higgs mass parameter and $m_h = 125$ GeV is the physical Higgs mass. In addition to the diagrams in Fig. 3, there is a logarithmic divergence due to stop mixing, as shown in Fig. 5. From these loops we find, for equal stop

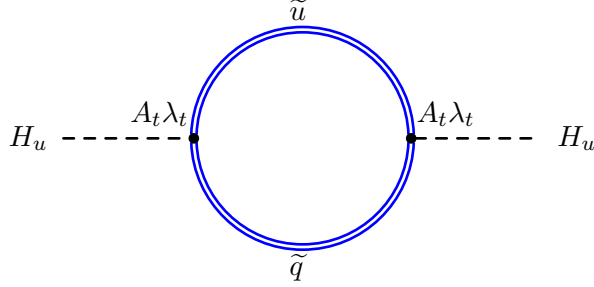


FIG. 5. Contribution to the logarithmic divergence in folded SUSY from the stop mixing term.

soft masses m_{soft} ,

$$|\delta m^2| = \frac{3\lambda_t^2}{16\pi^2} \left[2m_T^2 - 2m_t^2 - \frac{1}{2}m_Z^2 \cos 2\beta (1 + \hat{s}^2) + A_t^2 \right] \ln \left(\frac{\Lambda^2}{m_{\text{soft}}^2} \right) \quad (50)$$

where $\Lambda = 5$ TeV is the cutoff of the model. We have shown the tuning for various values of m_T^2 in Fig. 4. The color of each tuning contour corresponds to value of A_t used to generate the corresponding curve in the figure.

We see that the modifications to the Higgs couplings in Folded supersymmetry are very small, even when for very mild tuning. Therefore, precision Higgs couplings at the LHC will not strongly constrain naturalness. In this framework, however, top and quark partners are charged under electroweak interaction and will be produced. We therefore briefly investigate the collider limits on F-squarks.

C. Direct searches for F-squarks

Because the modifications to Higgs rates in folded supersymmetry are small, probes of naturalness in this framework may come from direct searches for F-squarks. Because of the new strong force, collider searches for F-squarks may be complicated by quirky dynamics [25]. The quirky narrative for folded SUSY has been outlined in [26]. The most promising signal comes from the production of an up-type and a down-type F-squark through an s-channel W . This pair of F-squarks is bound by a quirky string and forms an excited state which loses its excitation energy to soft radiation promptly on collider time scales. The exotic scalar meson, which is now in its ground state, is electrically charged and thus cannot decay into hidden glueballs. In [26] it was shown that the dominant decay of this state is prompt, going to $W\gamma$ with a branching ratio of about 0.85. The predicted signal of this framework is thus a $W\gamma$ resonance at twice the F-squark mass. We will now estimate the current limit

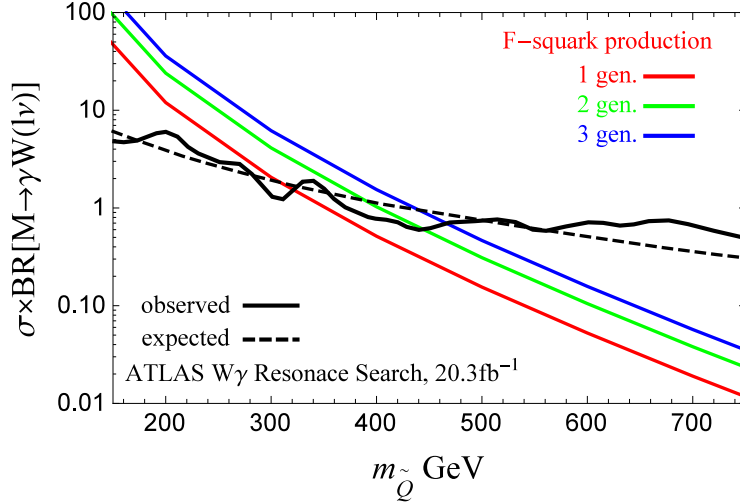


FIG. 6. An estimate of the ATLAS limits on the production of an up-down pair of F-squarks as a function of the F-squark mass, assuming 1, 2, or 3 such generations.

on this framework from an ATLAS $W\gamma$ resonance search [38].

To do this we make some simplifying assumptions. These assumptions lead to a best-case limit, and a more rigorous study is likely to yield weaker bounds. The mass splitting among these two states is expected to be small for the first two generation of F-squarks. Therefore, the time scale β decay of one into the other is expected to be longer than the time required for energy loss and decay. We assume that this is the case for the third generation as well.¹ We further assume that the contribution to the p_T of the ground state meson from energy loss is small, which would be the case if the radiation is perfectly isotropic (see [26] for corrections to this approximation). In this case the transverse mass peak is not smeared. Making these assumptions will give us an optimistic estimate for the limit.

The production cross section of the $W\gamma$ resonance is simply the cross section for up-down F-squark pair production. We calculate this cross section using MadGraph [39] at the 8 TeV LHC. Multiplying by the appropriate branching fractions, we compare this rate to the ATLAS limit in Fig. 6. We find that the estimated limits on the F-squark mass are about (320, 445, 465) GeV for 1, 2, and 3 generations respectively.

We conclude that natural models of folded supersymmetry are still allowed by current LHC searches, but future dedicated searches at run-II of the LHC are motivated. We also

¹ If this is not the case, β decay will precede the reannihilation of the F-squarks and the dominant channel is a pair of hidden glueballs.

note that depending on the dominant mechanism of energy loss, the $W\gamma$ resonance may be accompanied by many soft photons contributing to the underlying event [27].

IV. QUIRKY LITTLE HIGGS

A. The Model and Cancellation Mechanism

In Little Higgs models the Higgs doublet emerges as a pNGB whose mass is protected against one loop quadratic divergences by collective symmetry breaking. To understand how this mechanism operates, consider the Simplest Little Higgs model [7]. In this theory the $SU(2)_L \times U(1)_Y$ gauge symmetry of the SM is embedded in the larger gauge group $SU(3)_W \times U(1)_X$. All the states in the SM that are doublets under $SU(2)_L$ are now promoted to triplets. The Higgs sector for this theory is assumed to respect a larger approximate global $[SU(3) \times U(1)]^2$ symmetry, of which the gauged $SU(3)_W \times U(1)_X$ is a subgroup. This approximate global symmetry, which is explicitly violated by both the gauge and Yukawa interactions, is broken to $[SU(2) \times U(1)]^2$, which contains $SU(2)_L \times U(1)_Y$ of the SM as a subgroup. The SM Higgs doublet is contained among the uneaten pNGBs that emerge from this symmetry breaking pattern, and its mass is protected against large radiative corrections.

The symmetry breaking pattern may be realized using two scalar triplets of $SU(3)_W$, which we denote by ϕ_1 and ϕ_2 . If the tree level potential for these scalars, $V(\phi_1, \phi_2)$ is of the form

$$V(\phi_1, \phi_2) = V_1(\phi_1) + V_2(\phi_2) , \quad (51)$$

then this sector possesses an $[SU(3) \times U(1)]^2$ global symmetry. When ϕ_1 and ϕ_2 acquire VEVs f_1 and f_2 , this symmetry is broken to $[SU(2) \times U(1)]^2$. For simplicity we assume that the two VEVs are equal, so that $f_1 = f_2 = f$. However, this is not required for the mechanism to work. Of the 10 resulting NGBs, 5 are eaten while the remaining 5 contain the SM Higgs doublet.

The next step is to understand how the cancellation of quadratic divergences associated with the top Yukawa coupling arises in this theory. The top sector takes the form

$$\lambda_1 \phi_1 Q t_1 + \lambda_2 \phi_2 Q t_2 \quad (52)$$

where Q represents the $SU(3)$ triplet containing the third generation left-handed quarks,

while t_1 and t_2 are SU(3) singlets that carry the same electroweak charge as the right-handed top quark in the SM. These interactions do not respect the full $[\text{SU}(3) \times \text{U}(1)]^2$ global symmetry but only the gauged $\text{SU}(3)_W \times \text{U}(1)_X$ subgroup. As a consequence, the potential for ϕ_1 and ϕ_2 will receive corrections, and the 5 uneaten NGBs will acquire a mass. However, as we now explain, this radiatively generated contribution to the mass is not quadratically divergent, but only logarithmically divergent.

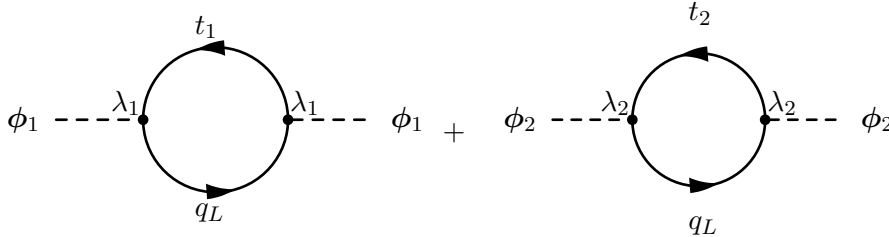


FIG. 7. Quadratic divergences from the top sector of the Littlest Higgs model.

The diagrams that can potentially lead to quadratically divergent contributions to the masses of the pNGBs are shown in Fig. 7. The divergent parts of these graphs are given by

$$\frac{3}{8\pi^2} \Lambda^2 \lambda_1^2 \phi_1^\dagger \phi_1 + \frac{3}{8\pi^2} \Lambda^2 \lambda_2^2 \phi_2^\dagger \phi_2. \quad (53)$$

However, we see that these terms respect the full global $\text{SU}(3) \times \text{SU}(3)$ symmetry and so cannot contribute to the mass of the pNGBs. This is not a coincidence, but a consequence of collective symmetry breaking. To see this, note that in (52) if either of the λ_i is set to zero then the Lagrangian for the top sector recovers the full $\text{SU}(3) \times \text{SU}(3)$ global symmetry and all the resulting NGBs are all massless. We see the global symmetry is violated only in the presence of both λ_1 and λ_2 , which collectively break the symmetry. Therefore, any correction to the pNGB masses can only arise from a diagram that includes both λ_1 and λ_2 . There are, however, no such quadratically divergent diagrams. The lowest order diagram that corrects the potential and contains both λ_1 and λ_2 is the box diagram, shown in Fig. 8, which is only logarithmically divergent.

We can show that this protection mechanism depends only on the symmetry breaking pattern of the model and is independent of the details of the dynamics that breaks the symmetry. To do this, we parametrize the uneaten pNGBs, in unitary gauge, by a set of fields $\pi(x)$. It is convenient to construct from the $\pi(x)$ two objects ϕ_1 and ϕ_2 that transform

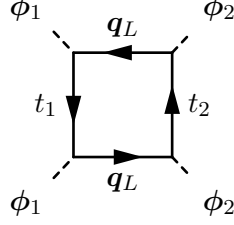


FIG. 8. Logarithmically divergent contribution to the Higgs potential. This contribution vanishes unless both λ_1 and λ_2 are nonzero.

linearly under the full broken $SU(3) \times SU(3)$ symmetry.

$$\varphi_1 = e^{i\Pi/f} \begin{pmatrix} 0 \\ 0 \\ f \end{pmatrix}, \quad \varphi_2 = e^{-i\Pi/f} \begin{pmatrix} 0 \\ 0 \\ f \end{pmatrix}, \quad (54)$$

with the relevant degrees of freedom encapsulated by

$$\Pi = \left(\begin{array}{cc|c} 0 & 0 & \mathbf{h} \\ 0 & 0 & \\ \hline \mathbf{h}^\dagger & & 0 \end{array} \right). \quad (55)$$

The Lagrangian for the top sector then takes the form

$$\frac{\lambda_1}{\sqrt{2}} \varphi_1^\dagger Q t_1 + \frac{\lambda_2}{\sqrt{2}} \varphi_2^\dagger Q t_2. \quad (56)$$

Expanding to quadratic order in \mathbf{h} and making the definitions

$$t^c \equiv i \left(\frac{\lambda_1}{\sqrt{\lambda_1^2 + \lambda_2^2}} t_2 - \frac{\lambda_1}{\sqrt{\lambda_1^2 + \lambda_2^2}} t_1 \right), \quad (57)$$

$$T^c \equiv \frac{\lambda_2}{\sqrt{\lambda_1^2 + \lambda_2^2}} t_2 + \frac{\lambda_1}{\sqrt{\lambda_1^2 + \lambda_2^2}} t_1 \quad (58)$$

this becomes

$$\mathbf{h} q (\lambda_t t^c + \lambda_T T^c) + m_T T T^c \left(1 - \frac{1}{2f^2} \mathbf{h}^\dagger \mathbf{h} \right). \quad (59)$$

Here we have defined

$$\lambda_t = \frac{\sqrt{2} \lambda_1 \lambda_2}{\sqrt{\lambda_1^2 + \lambda_2^2}}, \quad \lambda_T = i \frac{\lambda_2^2 - \lambda_1^2}{\sqrt{2} \sqrt{\lambda_1^2 + \lambda_2^2}}, \quad m_T = \frac{f}{\sqrt{2}} \sqrt{\lambda_1^2 + \lambda_2^2}. \quad (60)$$

The diagrams contributing to the Higgs mass, see Fig. 9, demonstrate the cancellation of quadratic divergences. Notice that because q couples to both t^c and T^c that the top partner

must transform under the same $SU(3)$ as the top. Thus, the two loops have been given the same color. If, however, there is some symmetry that forces $\lambda_1 = \lambda_2$ then the coupling λ_T of q to T^c vanishes and the cancellation can go through even if t^c and T^c transform under different $SU(3)$ color groups.

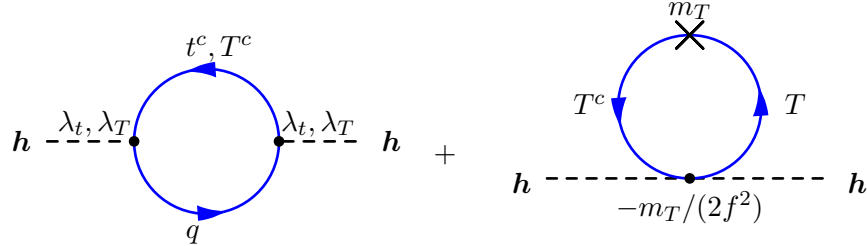


FIG. 9. Cancellation of quadratic divergences in the Littlest Higgs model. The two fermions must transform under the same $SU(3)$ unless $\lambda_1 = \lambda_2$.

In Quirky Little Higgs models the one loop quadratic divergences generated by the top quark are canceled exactly as in the diagrams shown above, but the fermionic top partners T and T^c do not transform under the SM color group, $SU(3)_c$. These partners are instead charged under a different $SU(3)$, called infracolor, and labeled as $SU(3)_{IC}$. However, the electroweak quantum numbers of the quirks are the same as those of their SM partners. In this construction, all the fermions that are charged under $SU(3)_{IC}$ have masses much above the scale where the gauge group gets strong. As a consequence, the system exhibits quirky dynamics.

Quirky Little Higgs models can be realized in a 5 dimensional space with the extra dimension compactified on S^1/Z_2 . The breaking of the $SU(3)_W \times U(1)_X$ gauge group down to the SM is realized by boundary conditions and separately by a scalar field Φ that transforms as a triplet under $SU(3)_W$. The 5 dimensional theory also possesses an $SU(6)$ gauge symmetry that is broken down to the SM $SU(3)$ color group and to $SU(3)_{IC}$ by boundary conditions. This construction allows the third generation quark doublet q and the top partner T to emerge as zero modes from the same bulk multiplet, but transforming under different color groups. The Higgs doublet is contained among the pNGBs that emerge from Φ after the breaking of the $SU(3)_W \times U(1)_X$ symmetry. The interactions in (59) arise from couplings of Φ to the multiplets that contain the top quarks and the top partners. The $SU(6)$ gauge symmetry ensures the equality of the couplings in (59) that is necessary to enforce the cancellation of the quadratic divergence.

B. Effects on Higgs Physics

When the scalar field Φ acquires a VEV, the $SU(3)_W \times U(1)_X$ gauge symmetry is broken down to $SU(2)_L \times U(1)_Y$ of the SM. We associate the SM-like Higgs doublet with some of the NGB modes that emerge from this breaking pattern. We parametrize the relevant degrees of freedom (neglecting the $SU(2)_W$ singlet that plays little role in the phenomenology) as

$$\Phi = \exp\left(\frac{i}{f}\Pi\right) \begin{pmatrix} 0 \\ 0 \\ f \end{pmatrix} \quad (61)$$

with

$$\Pi = \left(\begin{array}{cc|c} 0 & 0 & h_1 \\ 0 & 0 & h_2 \\ \hline h_1^* & h_2^* & 0 \end{array} \right). \quad (62)$$

Employing the symbol \mathbf{h} for the $SU(2)_W$ doublet of h_1 and h_2 we find

$$\Phi = \begin{pmatrix} \mathbf{h} \frac{if}{\sqrt{\mathbf{h}^\dagger \mathbf{h}}} \sin\left(\frac{\sqrt{\mathbf{h}^\dagger \mathbf{h}}}{f}\right) \\ f \cos\left(\frac{\sqrt{\mathbf{h}^\dagger \mathbf{h}}}{f}\right) \end{pmatrix}. \quad (63)$$

The top sector Yukawa interaction takes the form

$$-i \frac{\lambda_t f}{\sqrt{\mathbf{h}^\dagger \mathbf{h}}} \sin\left(\frac{\sqrt{\mathbf{h}^\dagger \mathbf{h}}}{f}\right) \mathbf{h}^\dagger t^c q + \lambda_t f \cos\left(\frac{\sqrt{\mathbf{h}^\dagger \mathbf{h}}}{f}\right) T T^c. \quad (64)$$

After moving to the unitary gauge $h_1 = 0$, $h_2 = (v + \rho)/\sqrt{2}$ this becomes

$$\lambda_t \left[-if \sin\left(\frac{v + \rho}{\sqrt{2}f}\right) t_L t^c + f \cos\left(\frac{v + \rho}{\sqrt{2}f}\right) T T^c \right] \quad (65)$$

with t_L and t^c transforming under $SU(3)$ color and T and T^c transforming under $SU(3)_{IC}$.

Expanding to first order in ρ and defining $\vartheta \equiv v/(\sqrt{2}f)$ we find

$$\begin{aligned} \lambda_t \left[-i \frac{v_{EW}}{\sqrt{2}} t_L t_R \left(1 + \frac{\rho}{v_{EW}} \cos \vartheta + \dots \right) \right. \\ \left. + f \cos \vartheta T T^c \left(1 - \frac{\rho}{v_{EW}} \tan \vartheta \sin \vartheta + \dots \right) \right] \end{aligned} \quad (66)$$

with $v_{EW} = \sqrt{2}f \sin \vartheta$. We see from this that the mass of the top and the mass of the top partner are related by $m_t = m_T \tan \vartheta$. The gauge sector analysis is very similar to that

of the A sector in MTH models. We expand the gauge kinetic term $|D_\mu \Phi|^2$ in the unitary gauge to find the couplings between ρ and the gauge bosons:

$$\left[m_W^2 W_\mu^+ W^{\mu-} + \frac{m_Z^2}{2} Z_\mu Z^\mu \right] \left(1 + 2 \frac{\rho}{v_{EW}} \cos \vartheta + \dots \right). \quad (67)$$

We see from this that all zero mode quark and gauge boson couplings are suppressed by a universal factor of $\cos \vartheta$ relative to the SM.

The fact that all the Higgs couplings are corrected by the same factor implies that all the production modes are also suppressed by a common factor relative to the SM,

$$\sigma(pp \rightarrow \rho) = \cos^2 \vartheta \sigma_{SM}(pp \rightarrow h). \quad (68)$$

A similar relation holds for all decay modes of the Higgs $\Gamma(\rho \rightarrow A_i)$, with the exception of $\Gamma(\rho \rightarrow \gamma\gamma)$, which receives new contributions from loops involving the top partners. The sign of the coupling of the top partner to the Higgs is opposite to that of the top. This causes their contributions to partially cancel, leading to an enhancement in the $\gamma\gamma$ rate. Using Eq. (A1) from Appendix A we find

$$\begin{aligned} \Gamma(\rho \rightarrow \gamma\gamma) = \frac{\alpha^2 m_\rho^3}{1024 \pi^3} & \left| \frac{2}{v_{EW}} \cos \vartheta A_V \left(\frac{4m_W^2}{m_\rho^2} \right) + \frac{2}{v_{EW}} \cos \vartheta \frac{4}{3} A_F \left(\frac{4m_t^2}{m_\rho^2} \right) \right. \\ & \left. - \frac{2}{\sqrt{2}f} \tan \vartheta \frac{4}{3} A_F \left(\frac{4m_T^2}{m_\rho^2} \right) \right|^2. \end{aligned} \quad (69)$$

We conclude that for all decay modes except the diphoton,

$$\frac{\sigma(pp \rightarrow \rho) \Gamma_{BR}(\rho \rightarrow A_i)}{\sigma_{SM}(pp \rightarrow h) \Gamma_{BR}^{SM}(h \rightarrow A_i)} = \frac{1}{1 + \frac{m_t^2}{m_T^2}}, \quad (70)$$

where we have neglected tiny effects of order $\Gamma(\rho \rightarrow \gamma\gamma)/\Gamma_{SM}(h)$. For diphoton decays

$$\frac{\sigma(pp \rightarrow \rho) \Gamma_{BR}(\rho \rightarrow \gamma\gamma)}{\sigma_{SM}(pp \rightarrow h) \Gamma_{BR}^{SM}(h \rightarrow \gamma\gamma)} = \frac{\Gamma(\rho \rightarrow \gamma\gamma)}{\Gamma_{SM}(h \rightarrow \gamma\gamma)}. \quad (71)$$

These functions are plotted in Fig. 10. The solid blue line denotes the rates for all final states other than diphoton and the dashed red line denotes the rate to diphotons. Note that even though the rate into two photons is enhanced because of the top partner loop, the universal suppression factor more than compensates for this, leading to a net suppression.

As with the MTH model, modification of Higgs couplings in the QLH model relative to the SM is constrained by precision electroweak measurements. The analysis of the MCHM4

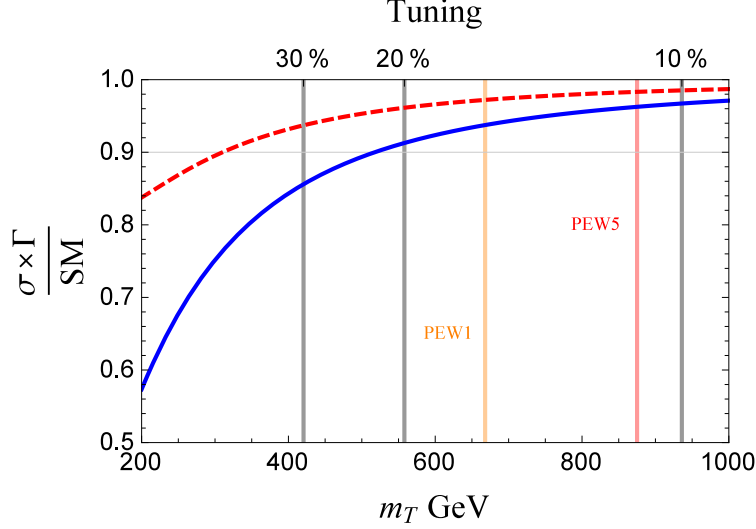


FIG. 10. Ratios of the rate of Higgs events into a given final state in Quirky Little Higgs model normalized to the SM. The solid blue line denotes the rates for all final states other than diphoton and the dashed red line denotes the diphoton final state. The vertical orange and red lines represent the 95% confidence bound from precision electroweak constraints at 1 and 5 TeV respectively.

model in [30] also applies to the QLH. Their bound on ϵ , where $\sqrt{1 - \epsilon^2} = \cos \vartheta$, can be translated into a bound on the top partner mass. This analysis was carried out assuming a cutoff $\Lambda = 3$ TeV. As in the MTH case, we can translate this bound on ϵ at Λ to a bound on ϵ' at Λ' ; see Eq. (32). The 2σ bound on ϵ' can be translated into a limit on the top partner mass. In Fig. 10 we denote the bound corresponding to a 1 and 5 TeV cutoff by the vertical orange and red lines respectively.

Finally, we estimate the tuning Δ_m of the Higgs mass parameter m^2 as a function of the top partner mass as a measure of the naturalness of the QLH model. We continue to use the formula

$$\Delta_m = \left| \frac{2\delta m^2}{m_h^2} \right|^{-1} \quad (72)$$

to estimate the tuning. We have denoted the quantum corrections to the Higgs mass parameter as δm^2 and the physical Higgs mass as $m_h = 125$ GeV.

The diagrams in Fig. 9, with $\lambda_1 = \lambda_2 = \lambda_t$ lead to

$$|\delta m^2| = \frac{3\lambda_t^2 m_T^2}{8\pi^2} \ln \left(\frac{\Lambda^2}{m_T^2} \right), \quad (73)$$

up to finite corrections. We take $\Lambda = 5$ TeV as the cutoff of the theory. In Fig. 10 we have labeled the top partner masses corresponding to 30%, 20%, and 10% tuning. We see again

that even at the 5% branching fraction precision expected at full luminosity, the LHC will not be able to probe tunings at the 10% level. Studies of the direct collider limits on quirky top partners are thus well motivated.

V. CONCLUSIONS

As the LHC bounds on new colored particles continue to grow, theories of physics beyond the SM that address the hierarchy problem with colorless top partners have become increasingly attractive. Since these new states must be light and couple to the Higgs with order one strength to address the hierarchy problem, their effects on Higgs production and decay can be significant. This suggests the possibility of using precision Higgs measurements at the LHC to probe these scenarios.

In this paper we have considered three theories of colorless top partners: the Mirror Twin Higgs, Folded Supersymmetry and the Quirky Little Higgs. In each case we determined the effects of the top partners on Higgs production and decay rates, and used the results to place limits on the top partner masses, and therefore on naturalness. We have shown that even with 3000 fb^{-1} at 14 TeV, the LHC will not be able to strongly disfavor naturalness.

ACKNOWLEDGMENTS

We thank Reinard Primulando and Tien-Tien Yu for discussions during early stages of this work. Z.C. and C.V. are supported by the National Science Foundation (NSF) Grant No. PHY-1315155. Fermilab is operated by Fermi Research Alliance, LLC under Contract No. DE-AC02-07CH11359 with the United States Department of Energy. R.H.'s work was supported in part by the NSF under Grant No. PHYS-1066293 and the hospitality of the Aspen Center for Physics. G.B. and L.L. acknowledge the support of the State of São Paulo Research Foundation (FAPESP). G.B. thanks the Brazilian National Council for Technological and Scientific Development (CNPq) for partial support and the University of Maryland Particle Theory group for its hospitality.

Appendix A: General Expressions for the Higgs Decay Rate to Two Photons

In all the models we consider, the effects of new physics on Higgs production and decays often occur as simply a multiplicative factor relative the SM. In tree level processes this is a reflection of modified couplings between the Higgs and SM fields. In loop mediated processes, however, we might expect more complicated corrections.

Because we are considering top partners which are not charged under color the gluon fusion and $h \rightarrow gg$ decay are affected in exactly the same way as tree level processes. When the top partner is electrically charged, however, the analysis of $h \rightarrow \gamma\gamma$ is more subtle.

At leading order the partial width of the Higgs to $\gamma\gamma$ is given by

$$\Gamma(h \rightarrow \gamma\gamma) = \frac{\alpha^2 m_h^3}{1024\pi^3} \left| \sum \mathcal{M} \right|^2 \quad (\text{A1})$$

where the amplitudes \mathcal{M} for each electrically charged vector, fermion, or scalar are given by

$$\mathcal{M}_V = \frac{g(m_V)}{m_V^2} Q_V^2 A_V(x_V), \quad (\text{A2})$$

$$\mathcal{M}_F = \frac{g(m_F)}{m_F^2} Q_F^2 A_F(x_F), \quad (\text{A3})$$

$$\mathcal{M}_S = \frac{g(m_S)}{m_S^2} Q_S^2 A_S(x_S). \quad (\text{A4})$$

In these definitions the Q s are the electrical charges in units of e , the charge of the proton and $g(m)$ is the coupling of the particle to the Higgs. The A functions are given by

$$A_V(x) = -x^2 \left[\frac{2}{x^2} + \frac{3}{x} + 3 \left(\frac{2}{x} - 1 \right) \arcsin^2 \left(\frac{1}{\sqrt{x}} \right) \right], \quad (\text{A5})$$

$$A_F(x) = 2x^2 \left[\frac{1}{x} + \left(\frac{1}{x} - 1 \right) \arcsin^2 \left(\frac{1}{\sqrt{x}} \right) \right], \quad (\text{A6})$$

$$A_S(x) = -x^2 \left[\frac{1}{x} - \arcsin^2 \left(\frac{1}{\sqrt{x}} \right) \right] \quad (\text{A7})$$

where $x_i = 4m_i^2/m_h^2$ and is understood to be greater than one. The couplings g are defined by

$$\frac{g(m)}{m^2} = \frac{1}{m^2(v)} \frac{\partial m^2(v)}{\partial v} \quad (\text{A8})$$

where in the case of fermions the mass squared is taken to mean $|m(v)|^2$.

Appendix B: MSSM with Extra $U(1)_X$

In this appendix we add a $U(1)_X$ gauge symmetry, with coupling g_X , to the MSSM which is then spontaneously broken. This affects the Higgs mass, the stop masses, and the Higgs couplings to the stops. We follow closely the work of [35].

All MSSM matter content is given equal charge under hypercharge and $U(1)_X$. In addition, the heavy scalar fields ϕ and ϕ^c , which spontaneously break the symmetry, carry charges $\pm q$ under the new $U(1)_X$ but are singlets under every other MSSM gauge group. These fields are part of chiral superfields Φ and Φ^c with superpotential

$$\mathcal{W} = \lambda S (\Phi \Phi^c - w^2) \quad (\text{B1})$$

and soft masses

$$m_\phi^2 (|\phi|^2 + |\phi^c|^2). \quad (\text{B2})$$

For $\lambda^2 w^2 > m_\phi^2$ and equal soft masses these scalars obtain identical nonzero VEVs $\langle \phi \rangle$. The $U(1)_X$ gauge field Z'_μ also gets a mass $m_{Z'} = 2qg_X \langle \phi \rangle$.

The usual MSSM D -terms

$$\frac{g_L^2}{2} \left(\sum_{\text{MSSM}} \phi_i^* q_i \sigma^a \phi_i \right)^2 + \frac{g_Y^2}{2} \left(\sum_{\text{MSSM}} \phi_i^* q_i \phi_i \right)^2 \quad (\text{B3})$$

(with the q_i denoting the charge of the i th field with respect to the appropriate gauge symmetry) are joined by

$$\frac{g_X^2}{2} \left(\sum_{\text{MSSM}} \phi_i^* q_i \phi_i + q|\phi|^2 - q|\phi^c|^2 \right)^2. \quad (\text{B4})$$

When ϕ and ϕ^c have masses much higher than the weak scale we can integrate them out. This generates the leading D -terms

$$\frac{g_L^2}{2} \left(\sum_{\text{MSSM}} \phi_i^* q_i \sigma^a \phi_i \right)^2 + \frac{g_Y^2 + \hat{g}^2}{2} \left(\sum_{\text{MSSM}} \phi_i^* q_i \phi_i \right)^2 \quad (\text{B5})$$

where

$$\hat{s}^2 = g_X^2 \left(1 + \frac{m_{Z'}^2}{2m_\phi^2} \right)^{-1} \frac{v_{\text{EW}}^2}{4m_Z^2}. \quad (\text{B6})$$

This effective enhancement of the hypercharge D -term raises the tree level Higgs mass to

$$m_{h^0}^2 = m_Z^2 \cos^2 2\beta (1 + \hat{s}^2). \quad (\text{B7})$$

The D -term contributions to the Higgs-stop couplings and the stop masses are similarly modified, as shown in the body of the paper. All numerical results, see Fig. 4, use the value of \hat{s} such that $m_{h^0} = 125$ GeV with stop loop corrections to the Higgs mass included[3]:

$$m_{h^0}^2 = m_Z^2 \cos^2 2\beta (1 + \hat{s}^2) + \frac{3\lambda_t^2 \sin^2 \beta}{2\pi^2} \left\{ m_t^2 \ln \left(\frac{m_{\tilde{T}} m_{\tilde{t}}}{m_t^2} \right) + \frac{\sin^2 2\alpha_t}{4} (m_{\tilde{T}}^2 - m_{\tilde{t}}^2) \ln \left(\frac{m_{\tilde{T}}^2}{m_{\tilde{t}}^2} \right) \right. \\ \left. + \frac{\sin^4 2\alpha_t}{16m_t^2} \left[(m_{\tilde{T}}^2 - m_{\tilde{t}}^2)^2 - \frac{1}{2} (m_{\tilde{T}}^4 - m_{\tilde{t}}^4) \ln \left(\frac{m_{\tilde{T}}^2}{m_{\tilde{t}}^2} \right) \right] \right\} \quad (\text{B8})$$

where we have used the definition of $\sin 2\alpha_t$ from (41).

-
- [1] G. Aad *et al.* (ATLAS Collaboration), Phys.Lett. **B716**, 1 (2012), arXiv:1207.7214 [hep-ex].
 - [2] S. Chatrchyan *et al.* (CMS Collaboration), Phys.Lett. **B716**, 30 (2012), arXiv:1207.7235 [hep-ex].
 - [3] S. P. Martin, (1997), arXiv:hep-ph/9709356 [hep-ph].
 - [4] N. Arkani-Hamed, A. G. Cohen, and H. Georgi, Phys.Lett. **B513**, 232 (2001), arXiv:hep-ph/0105239 [hep-ph].
 - [5] N. Arkani-Hamed, A. Cohen, E. Katz, A. Nelson, T. Gregoire, *et al.*, JHEP **0208**, 021 (2002), arXiv:hep-ph/0206020 [hep-ph].
 - [6] N. Arkani-Hamed, A. Cohen, E. Katz, and A. Nelson, JHEP **0207**, 034 (2002), arXiv:hep-ph/0206021 [hep-ph].
 - [7] M. Schmaltz, JHEP **0408**, 056 (2004), arXiv:hep-ph/0407143 [hep-ph].
 - [8] M. Schmaltz and D. Tucker-Smith, Ann.Rev.Nucl.Part.Sci. **55**, 229 (2005), arXiv:hep-ph/0502182 [hep-ph].
 - [9] S. Chatrchyan *et al.* (CMS Collaboration), Eur.Phys.J. **C73**, 2677 (2013), arXiv:1308.1586 [hep-ex].
 - [10] CMS-PAS-SUS-14-011 (CMS Collaboration), (2014).
 - [11] G. Aad *et al.* (ATLAS Collaboration), (2014), arXiv:1407.0583 [hep-ex].
 - [12] G. Aad *et al.* (ATLAS Collaboration), JHEP **1409**, 015 (2014), arXiv:1406.1122 [hep-ex].
 - [13] S. P. Martin, Phys.Rev. **D75**, 115005 (2007), arXiv:hep-ph/0703097 [HEP-PH].
 - [14] J. Fan, M. Reece, and J. T. Ruderman, JHEP **1111**, 012 (2011), arXiv:1105.5135 [hep-ph].

- [15] Z. Chacko, H.-S. Goh, and R. Harnik, Phys.Rev.Lett. **96**, 231802 (2006), arXiv:hep-ph/0506256 [hep-ph].
- [16] G. Burdman, Z. Chacko, H.-S. Goh, and R. Harnik, JHEP **02**, 009 (2007), arXiv:hep-ph/0609152 [hep-ph].
- [17] D. Poland and J. Thaler, JHEP **0811**, 083 (2008), arXiv:0808.1290 [hep-ph].
- [18] H. Cai, H.-C. Cheng, and J. Terning, JHEP **05**, 045 (2009), arXiv:0812.0843 [hep-ph].
- [19] R. Barbieri, T. Gregoire, and L. J. Hall, (2005), arXiv:hep-ph/0509242 [hep-ph].
- [20] Z. Chacko, Y. Nomura, M. Papucci, and G. Perez, JHEP **0601**, 126 (2006), arXiv:hep-ph/0510273 [hep-ph].
- [21] S. Chang, L. J. Hall, and N. Weiner, Phys.Rev. **D75**, 035009 (2007), arXiv:hep-ph/0604076 [hep-ph].
- [22] N. Craig and K. Howe, JHEP **1403**, 140 (2014), arXiv:1312.1341 [hep-ph].
- [23] N. Craig, S. Knapen, and P. Longhi, (2014), arXiv:1410.6808 [hep-ph].
- [24] M. J. Strassler and K. M. Zurek, Phys.Lett. **B651**, 374 (2007), arXiv:hep-ph/0604261 [hep-ph].
- [25] J. Kang and M. A. Luty, JHEP **0911**, 065 (2009), arXiv:0805.4642 [hep-ph].
- [26] G. Burdman, Z. Chacko, H.-S. Goh, R. Harnik, and C. A. Krenke, Phys.Rev. **D78**, 075028 (2008), arXiv:0805.4667 [hep-ph].
- [27] R. Harnik and T. Wizansky, Phys.Rev. **D80**, 075015 (2009), arXiv:0810.3948 [hep-ph].
- [28] A. Djouadi, Physics Reports **457**, 1 (2008), arXiv:hep-ph/05031720 [hep-ph].
- [29] S. Heinemeier, C. Mariotti, G. Passarino, and R. Tanaka (LHC Higgs Cross Section Working Group), CERN2013004 (2013), arXiv:1307.1347 [hep-ph].
- [30] A. Falkowski, F. Riva, and A. Urbano, JHEP **1311**, 111 (2013), arXiv:1303.1812 [hep-ph].
- [31] K. Agashe, R. Contino, and A. Pomarol, Nucl.Phys. **B719**, 165 (2005), arXiv:hep-ph/0412089 [hep-ph].
- [32] S. Dawson, A. Gritsan, H. Logan, J. Qian, C. Tully, *et al.*, (2013), arXiv:1310.8361 [hep-ex].
- [33] N. Craig and H. K. Lou, (2014), arXiv:1406.4880 [hep-ph].
- [34] H. E. Haber, (1993), arXiv:hep-ph/9306207 [hep-ph].
- [35] P. Batra, A. Delgado, D. E. Kaplan, and T. M. Tait, JHEP **0402**, 043 (2004), arXiv:hep-ph/0309149 [hep-ph].
- [36] K. Olive *et al.* (Particle Data Group), Chin.Phys. **C38**, 090001 (2014).

- [37] J. Fan and M. Reece, JHEP **1406**, 031 (2014), arXiv:1401.7671 [hep-ph].
- [38] G. Aad *et al.* (ATLAS Collaboration), Phys.Lett. **B738**, 428 (2014), arXiv:1407.8150 [hep-ex].
- [39] J. Alwall, M. Herquet, F. Maltoni, O. Mattelaer, and T. Stelzer, JHEP **1106**, 128 (2011), arXiv:1106.0522 [hep-ph].